



## **LASER VELOCIMETER UTILIZATION IN JET ENGINE ALTITUDE TEST CELLS**

**ENGINE TEST FACILITY  
ARNOLD ENGINEERING DEVELOPMENT CENTER  
AIR FORCE SYSTEMS COMMAND  
ARNOLD AIR FORCE STATION, TENNESSEE 37389**

**June 1977**

**Final report for Period October 1975 — June 1976**

Approved for public release; distribution unlimited.

**Prepared for:**

**DIRECTORATE OF TECHNOLOGY (DY)  
ARNOLD ENGINEERING DEVELOPMENT CENTER  
ARNOLD AIR FORCE STATION, TENNESSEE 37389**

## NOTICES

When U. S. Government drawings specifications, or other data are used for any purpose other than a definitely related Government procurement operation, the Government thereby incurs no responsibility nor any obligation whatsoever, and the fact that the Government may have formulated, furnished, or in any way supplied the said drawings, specifications, or other data, is not to be regarded by implication or otherwise, or in any manner licensing the holder or any other person or corporation, or conveying any rights or permission to manufacture, use, or sell any patented invention that may in any way be related thereto.

Qualified users may obtain copies of this report from the Defense Documentation Center.

References to named commercial products in this report are not to be considered in any sense as an endorsement of the product by the United States Air Force or the Government.

This report has been reviewed by the Information Office (OI) and is releasable to the National Technical Information Service (NTIS). At NTIS, it will be available to the general public, including foreign nations.

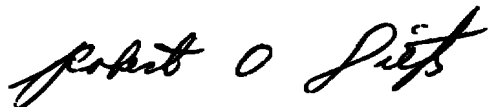
## APPROVAL STATEMENT

This technical report has been reviewed and is approved for publication.

FOR THE COMMANDER



MARSHALL K. KINGERY  
Research & Development  
Division  
Directorate of Technology



ROBERT O. DIETZ  
Director of Technology

# UNCLASSIFIED

REPORT DOCUMENTATION PAGE		READ INSTRUCTIONS BEFORE COMPLETING FORM
1. REPORT NUMBER <b>AEDC-TR-77-21</b>	2. GOVT ACCESSION NO.	3. RECIPIENT'S CATALOG NUMBER
4. TITLE (and Subtitle) <b>LASER VELOCIMETER UTILIZATION IN JET ENGINE ALTITUDE TEST CELLS</b>	5. TYPE OF REPORT & PERIOD COVERED <b>Final Report-October 1975-June 1976</b>	
	6. PERFORMING ORG. REPORT NUMBER	
7. AUTHOR(s)  <b>D. O. Barnett and D. B. Brayton, ARO, Inc.</b>	8. CONTRACT OR GRANT NUMBER(s)	
9. PERFORMING ORGANIZATION NAME AND ADDRESS <b>Arnold Engineering Development Center (DY) Air Force Systems Command Arnold Air Force Station, Tennessee 37389</b>	10. PROGRAM ELEMENT, PROJECT, TASK AREA & WORK UNIT NUMBERS <b>Program Element 65807F</b>	
11. CONTROLLING OFFICE NAME AND ADDRESS <b>Arnold Engineering Development Center (DYFS), Arnold Air Force Station, Tennessee 37389</b>	12. REPORT DATE <b>June 1977</b>	
	13. NUMBER OF PAGES <b>33</b>	
14. MONITORING AGENCY NAME & ADDRESS (if different from Controlling Office)	15. SECURITY CLASS. (of this report)  <b>UNCLASSIFIED</b>	
	15a. DECLASSIFICATION/DOWNGRADING SCHEDULE <b>N/A</b>	
16. DISTRIBUTION STATEMENT (of this Report)  <b>Approved for public release; distribution unlimited.</b>		
17. DISTRIBUTION STATEMENT (of the abstract entered in Block 20, if different from Report)		
18. SUPPLEMENTARY NOTES  <b>Available in DDC</b>		
19. KEY WORDS (Continue on reverse side if necessary and identify by block number) <b>laser velocimeters      altitude      vibration flow field      test facilities      temperature measurements      control jet engine      environments</b>		
20. ABSTRACT (Continue on reverse side if necessary and identify by block number)  <b>The feasibility of utilizing a laser velocimeter (LV) in turbine engine testing in an altitude test cell was investigated. A one-component LV and associated environmental control system (ECS) were designed, fabricated, and installed in Test Cell J-2 of the Engine Test Facility (ETF). LV measurements made on the centerline of an F101 engine at one axial station downstream of the nozzle exit are presented and compared to the calculated exit</b>		

# UNCLASSIFIED

# UNCLASSIFIED

## 20. ABSTRACT (Continued)

velocity. Design data are presented on the vibration levels and temperatures encountered by the LV over a range of engine operating conditions. It was found that sufficient natural seed material existed in the exhaust flow to allow the LV to characterize the exit velocity of a turbojet engine during altitude testing.

UNCLASSIFIED

## **PREFACE**

The work reported herein was conducted by the Arnold Engineering Development Center (AEDC), Air Force Systems Command (AFSC), under Program Element 65807F. The results were obtained by ARO, Inc., AEDC Division (a Sverdrup Corporation Company), operating contractor for the AEDC, AFSC, Arnold Air Force Station, Tennessee. The work was done under ARO Projects No. R32P and P32S. The authors of this report were D. O. Barnett and D. B. Brayton, ARO, Inc. The manuscript (ARO Control No. ARO-ETF-TR-76-147) was submitted for publication on December 17, 1976.

## CONTENTS

	<u>Page</u>
1.0 INTRODUCTION	
1.1 Background . . . . .	5
1.2 Scope of Investigation . . . . .	7
2.0 EXPERIMENTAL APPARATUS AND PROCEDURES	
2.1 Engine Installation . . . . .	8
2.2 Laser Velocimeter and Environmental Control Systems . . . . .	10
2.3 Supporting Instrumentation . . . . .	14
2.4 Data Acquisition Systems . . . . .	15
2.5 Instrument Uncertainty . . . . .	15
2.6 Test Procedures . . . . .	16
2.7 Data Reduction . . . . .	17
3.0 RESULTS AND DISCUSSION	
3.1 Environmental Data . . . . .	18
3.2 Laser Velocimeter Utilization . . . . .	22
4.0 CONCLUSIONS . . . . .	26
REFERENCES . . . . .	27

## ILLUSTRATIONS

### Figure

1. F101 Engine Installation in Propulsion Development Test Cell (J-2) . . . . .	9
2. LV Optical Arrangement . . . . .	10
3. LV/ECS Installation . . . . .	12
4. ECS/Test Cell Installation . . . . .	13
5. Axial Acceleration-Frequency Distribution . . . . .	20
6. Transverse Acceleration-Frequency Distribution . . . . .	20
7. Vertical Acceleration-Frequency Distribution . . . . .	20
8. Exit Velocity Histogram for Engine Idle . . . . .	24
9. Exit Velocity Histogram for Intermediate Power . . . . .	24
10. Exit Velocity Histogram for Maximum Thrust Augmentation . . . . .	25

## TABLES

1. Maximum Acceleration/Frequency Levels . . . . .	21
2. Lens/ECS Compartment Temperatures . . . . .	21
3. Comparison of Measured and Computed Mean Velocities . . . . .	26

**APPENDIX**

**A. LV ALIGNMENT CHARACTERISTICS . . . . . 29**

**NOMENCLATURE . . . . . 32**

## 1.0 INTRODUCTION

The ability to determine the spatial and temporal variation of fluid velocity would be of benefit in many development and performance tests of aerospace propulsion systems. For example, mean velocity data could be used to (1) evaluate the directionality and swirl characteristics of an exhaust flow or (2) provide an independent measurement of thrust when used in conjunction with temperature and pressure data. In addition, details of the local turbulence structure can be derived from velocity measurements to provide insight into the fluid mechanics, chemistry, and acoustic and thermal radiation properties of propulsive flows.

The flows associated with turbojet, ramjet, or rocket propulsion systems, however, are typified by high velocities and temperatures so that conventional instrumentation such as hot-wire anemometers or pitot probes are subject to damage from impact or thermal loadings imposed by the fluid environment. Such material probes, moreover, introduce flow disturbances so that their use may be undesirable even when the pressure loadings and thermal stresses can be tolerated. These difficulties are avoided by the laser velocimeter (LV) which remotely measures velocity and, consequently, does not directly interact with the flow being studied. The many recent applications of LV systems to a wide variety of practical flow problems (Refs. 1 through 3) suggest, additionally, that the laser velocimeter has the potential of providing accurate local velocity data in propulsive flows. To successfully accomplish this objective, however, requires careful consideration of constraints imposed by testing in an engine test cell environment as well as certain fundamental limitations of LV systems.

### 1.1 BACKGROUND

An LV measures the Doppler shift of light scattered by particles traversing a probe volume. If the particles are small enough to respond to variations in the velocity of the fluid in which they are contained, extremely accurate measurements of gas or liquid velocity can be obtained.

The major subsystems of an LV may be categorized as (1) a laser (which provides a coherent, highly collimated light source), (2) illuminating optics (which precondition and focus the laser radiation to form the probe volume), (3) detector optics (which collect and focus light scattered by particles moving through the probe volume), and (4) signal conditioning electronics (which amplify the scattered radiation and process the signal to obtain a Doppler frequency). The specification and arrangement of the components associated with the preceding subsystems are dictated by the intended application of the LV.



At the Arnold Engineering Development Center (AEDC), gas turbine engine and rocket tests are performed in chambers designed to simulate altitude and external flow conditions that will be encountered in the flight envelope of the aircraft or missile system for which the propulsion unit was developed. Within these altitude chambers, radiative heat fluxes may be high, and support structures experience mechanically and/or acoustically induced vibrations. Consequently, an LV system mounted within the cell must be protected from the cell environment even though it does not come in contact with flow from the propulsion system. Thus, an environmental control system (ECS) is required that will (1) maintain sufficiently high pressures in the vicinity of the laser so that electrical breakdown of the plasma tube does not occur, (2) protect the optical system from localized aerodynamic loads in the cells that would adversely affect the LV radiation alignment, (3) control temperatures in the vicinity of optical and electrical components to prevent thermally induced component failures, and (4) provide sufficient vibration isolation so that component integrity is preserved and radiation alignment maintained. Oil or fuel spills are not uncommon during a test program, and attention must be given to preserving the integrity of exposed optical components to prevent signal degradation caused by surface contamination.

To simplify the ECS design, it is desirable to arrange the LV optics so that the angle between the normals to the illuminating and scattered wavefronts is less than  $\pm\pi/2$ . By using such a backscatter arrangement, both the illuminating and detector optics can be placed in a single compartment. Backscatter systems, moreover, are less likely to lose radiation alignment because of random structural vibrations and are more compact so that traversing the system to reposition the probe volume is easier. It should be noted, however, that light scattering efficiencies are lower in the backscatter mode and high laser power is required to permit detection of small particles.

While providing adequate environmental protection will ensure the operational integrity of an LV in a test cell environment, the accuracy of the data to be obtained is strongly influenced by the size distribution and concentration of particles in the engine exhaust flow. To obtain accurate gas velocity measurements, particle sizes must be small relative to the scale of the experiment (Ref. 4), yet large enough to scatter sufficient light for processing by the LV electronics. For efficient operation of an LV, particle concentrations must be high enough that sufficient particles pass through the probe volume to allow a measurement to be obtained in a reasonable time, but low enough that only one particle is in the probe volume at any time. These limitations on the characteristics of the particle field can be met if the flow is seeded with particles of a controlled size. Seeding is not a satisfactory solution for testing of propulsion devices since the introduction of foreign matter to the turbine engine may cause damage to the engine or create an uncertainty in the validity of engine performance data. It is desirable,

therefore, to obtain LV measurements from particulates which occur naturally in an engine exhaust flow. Although particle characteristics, size and distribution, will not generally be known for a specific application, it is possible to estimate their influence on LV performance from published studies.

Broderick (Ref. 5) has measured the distribution of particle sizes in the exhaust flow of a turbojet engine installed in the AEDC Propulsion Development Test Cell (J-2) of the Engine Test Facility. He found that 99.9 percent of the particles were less than  $0.5\ \mu\text{m}$  in diameter and that 50 percent had diameters less than  $0.05\ \mu\text{m}$ . Particle lag effects are usually negligible for submicron particles and, if these data are typical of turbojet exhausts, an LV should provide accurate estimates of engine exit velocity. Conversely, the particle size data are heavily weighted to particle sizes ( $d_p \ll 0.2\ \mu\text{m}$ ) that will yield photon-limited Doppler signals (Ref. 6), so that most particles will not produce signals which can be analyzed with conventional frequency processors. Although velocity measurements can be made in flows dominated by photon-limited signals through the use of photon correlation techniques (Ref. 7), it is necessary to consider the particle concentration before discarding the more conventional approach to the problem.

Experiments conducted in a gas turbine combustor (Ref. 8) showed that the particulates contained in the exhaust gas were predominantly carbon particles. Typically, the effluent had a particulate concentration of  $0.0028\ \text{g/m}^3$ . For gas velocity of 1,500 fps and an ellipsoidal probe volume 10 mm in length by 0.5 mm in diameter; the volumetric flow rate through the probe volume is  $0.0018\ \text{m}^3/\text{sec}$ . For an average particle diameter of  $0.10\ \mu\text{m}$  and density of  $2\ \text{g/cc}$ , the average number of particles traversing the probe volume is about  $5 \times 10^9$  particles/sec. Clearly, if only one particle in  $10^7$  yields a photon-resolved signal, a data rate near 500 samples/sec would be possible using, for example, burst data processors (Ref. 9). Such a data rate is compatible with making one or more velocity measurements while the engine is at a test condition. It should be noted, however, that for particle size and concentrations comparable to the above, the probability is high that many particles will occupy the probe volume during the transit time of a detectable particle. It has been shown (Ref. 10) that LV signals obtained with many particles in the probe volume can be extremely noisy and it becomes uncertain whether the signal-to-noise (S/N) ratio of a typical Doppler burst would be high enough to allow the signal to be processed.

## 1.2 SCOPE OF INVESTIGATION

An experimental program was conducted in Propulsion Development Test Cell (J-2) to determine the feasibility of using an LV to obtain velocity measurements for a gas turbine engine without seeding the engine flow. The objectives of the study were to design

an LV and an ECS suitable for use in an engine altitude test cell, ascertain whether enough processable Doppler signals could be obtained during engine steady-state operation to make LV utilization practical and, if successful in the above, to make comparisons between the LV measurements and theoretical calculations of the engine exhaust velocity.

To achieve these objectives a one-component, backscatter LV and associated ECS were designed and tested during F101 engine performance evaluations. LV system vibration and temperature data were obtained and are presented for engine power settings from idle to maximum thrust augmentation at altitudes from sea level to 55,000 ft. LV measurements of the centerline velocity and turbulence intensity at various engine power settings are presented for an axial location 0.1 nozzle diameters downstream of the nozzle exit plane.

## 2.0 EXPERIMENTAL APPARATUS AND PROCEDURES

### 2.1 ENGINE INSTALLATION

The test article to which the LV development program was directed was an F101-GE-100 dual-spool, axial-flow turbofan engine. The engine consists of a two-stage fan, a nine-stage high-pressure compressor, turbine frame, mixer, augmentor, and a primary and secondary variable-area exhaust nozzle. It is a 30,000-lb-thrust-class engine with a corrected airflow rate of 350 lbm/sec and a 2:1 bypass ratio. The engine was installed in the AEDC Propulsion Development Test Cell (J-2) (Ref. 11) which has a 20-ft-diam by 69-ft-long test section. The test cell is capable of providing airflow rates up to 675 lbm/sec at engine air inlet temperatures ranging from -10 to +750°F. Simulated pressure altitudes up to 80,000 ft can be provided by the facility exhaust compressors. Figure 1 shows the F101 engine installed in the test cell.

The engine exhaust flow is removed from the test cell through a 6-ft-diam, water-cooled diffuser extension located 14 in. downstream of the engine exit plane. Because of the proximity of the diffuser to the engine and the location of existing viewing ports, observations of the engine exhaust plane could not be obtained from outside the cell. It was necessary, therefore, to install the laser velocimeter within the cell to obtain measurements of the engine exhaust velocity. Positioning the LV closer to the engine provided a greater optical collection efficiency and increased the possibility of obtaining meaningful velocity data, although this approach required the design of an ECS to protect the instrument from extremes in pressure, temperature, and vibration.

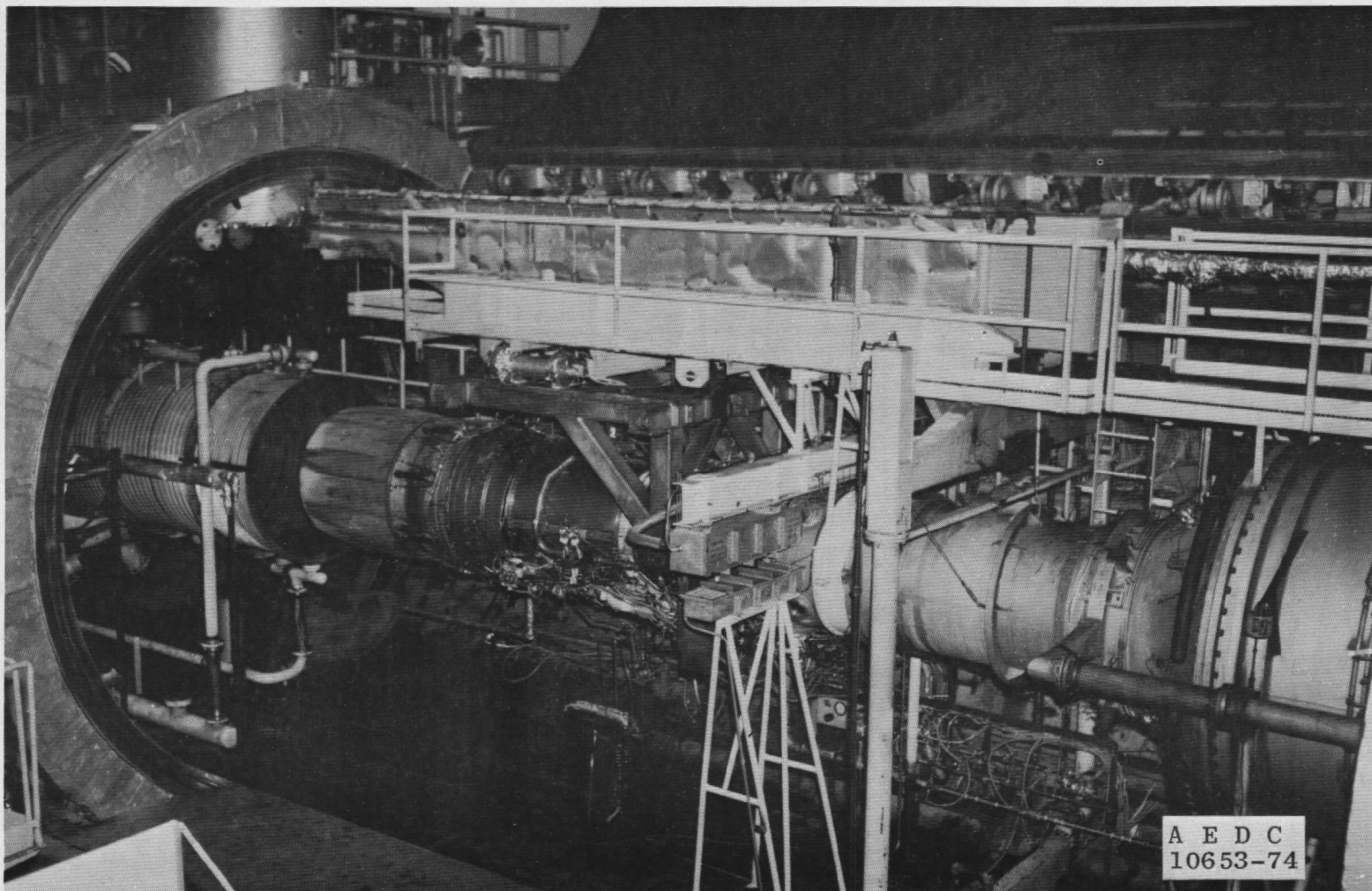


Figure 1. F101 engine installation in Propulsion Development Test Cell (J-2).

## 2.2 LASER VELOCIMETER AND ENVIRONMENTAL CONTROL SYSTEMS

A one-component, on-axis, backscatter LV was used in the test program. The optical configuration is depicted in Fig. 2. A detailed discussion of the LV optical alignment, alignment detection, and baffling is presented in Appendix A. To achieve compactness, the optical axis was folded. Light from a nominally, 0.7-watt argon-ion laser was directed by a mirror,  $M_1$ , through the beam expander, BE, onto a second mirror,  $M_2$ , which redirected the expanded laser beam to a beam splitter, BS. Two equal intensity, parallel rays emerged from the beam splitter, were turned by mirror,  $M_3$ , and focused by the central portion of the transmitter lens,  $L_1$ , to form a probe volume, P, located at the lens focal point.

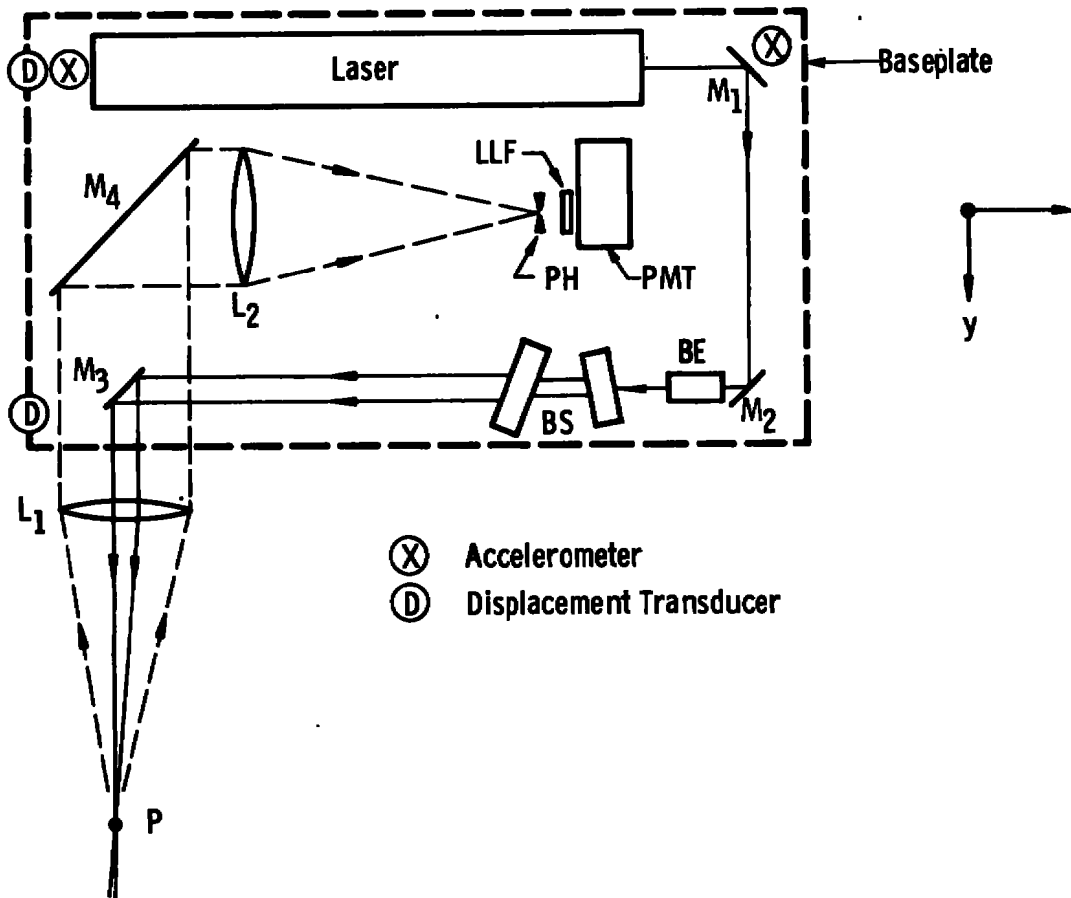


Figure 2. LV optical arrangement.

Because of interference between the intersecting beams, a system of stationary fringes was formed in the probe volume. Two transmitter lenses having focal lengths of 30 and 48 in., respectively, were used in the test series. For the 30-in. focal length lens the fringe spacing,  $\delta$ , was  $17.6 \mu\text{m}$  giving a velocity-to-frequency ratio,  $K_v$ , of 57.7

fps/MHz, whereas for the 48-in. lens,  $\delta = 27.6 \mu\text{m}$  and  $K_v = 90.7 \text{ fps/MHz}$ . The probe volume formed by an LV of this configuration is an ellipsoid of revolution oriented so that its major axis,  $a$ , is parallel to the engine exit plane and its minor axis,  $b$ , is parallel to the flow direction. The dimensions of the geometric probe volume (Ref. 12) defined by the  $\pm 1/e^2$  intensity contours were  $a = 20.9 \text{ mm}$  and  $b = 0.29 \text{ mm}$  for the 30-in. focal length lens, whereas for the 48-in. lens,  $a = 49.7 \text{ mm}$  and  $b = 0.44 \text{ mm}$ .

Light scattered from particles traversing the probe volume was collected by the lens  $L_1$  and redirected by the mirror,  $M_4$ , to the lens  $L_2$  which focused the collected radiation through a circular aperture, (pinhole, PH), onto a photomultiplier tube, PMT. To minimize the background radiation received from the engine and cell lighting, a laser line filter, LLF, was used to exclude radiation contributed by wavelengths other than the 514.5-nm line in which the laser was operated. Possible interference between the illuminating and scattered radiation was minimized by a series of baffles (Fig. 3) located between the input and collector branches of the LV system. No provisions were made to remotely align the collector optics, but an alignment detection system (see Appendix A) was used to determine whether or not alignment was maintained throughout a test condition.

The optical components, PMT, and an amplifier were installed in an ECS consisting of an insulated compartment, vibration isolated mounting plate, pressurization system, and heat shield. The assembled LV/ECS package is shown in Figs. 3 and 4. The compartment was 72 in. by 30 in. by 15 in. with a 7.5-in.-diam by 18.5-in.-long cylindrical extension which housed the transmitting lens. Access to the collector optics was obtained through a removable side plate, and the entire system was accessible from the top of the compartment. All LV optics except the transmitting lens were mounted on a baseplate which contained four optical rails along which the components were mounted. The baseplate was attached to the compartment by pneumatic vibration isolators located at each corner. This arrangement reduced the resonant frequency of the baseplate/optical assembly to less than 1 Hz. A passive pressurization system was used with pressure being maintained by venting the ECS compartment to the atmosphere through the hoses seen in Fig. 4. Limited temperature control was obtained by a cold gaseous nitrogen ( $\text{GN}_2$ ) purge, insulation, and a water-cooled heat shield (Fig. 4) installed between the ECS and engine exhaust. A portion of the  $\text{GN}_2$  flow was diverted through the transmitter lens housing to purge the exposed surface of the lens and to provide additional cooling. Electrical leads, laser cooling water, and instrumentation leads were routed to the compartment through the vent lines. For this feasibility study, the LV was not provided with a traversing capability but, in the event of overheating or a structural failure, it could be retracted along rails by a pneumatically actuated piston assembly.



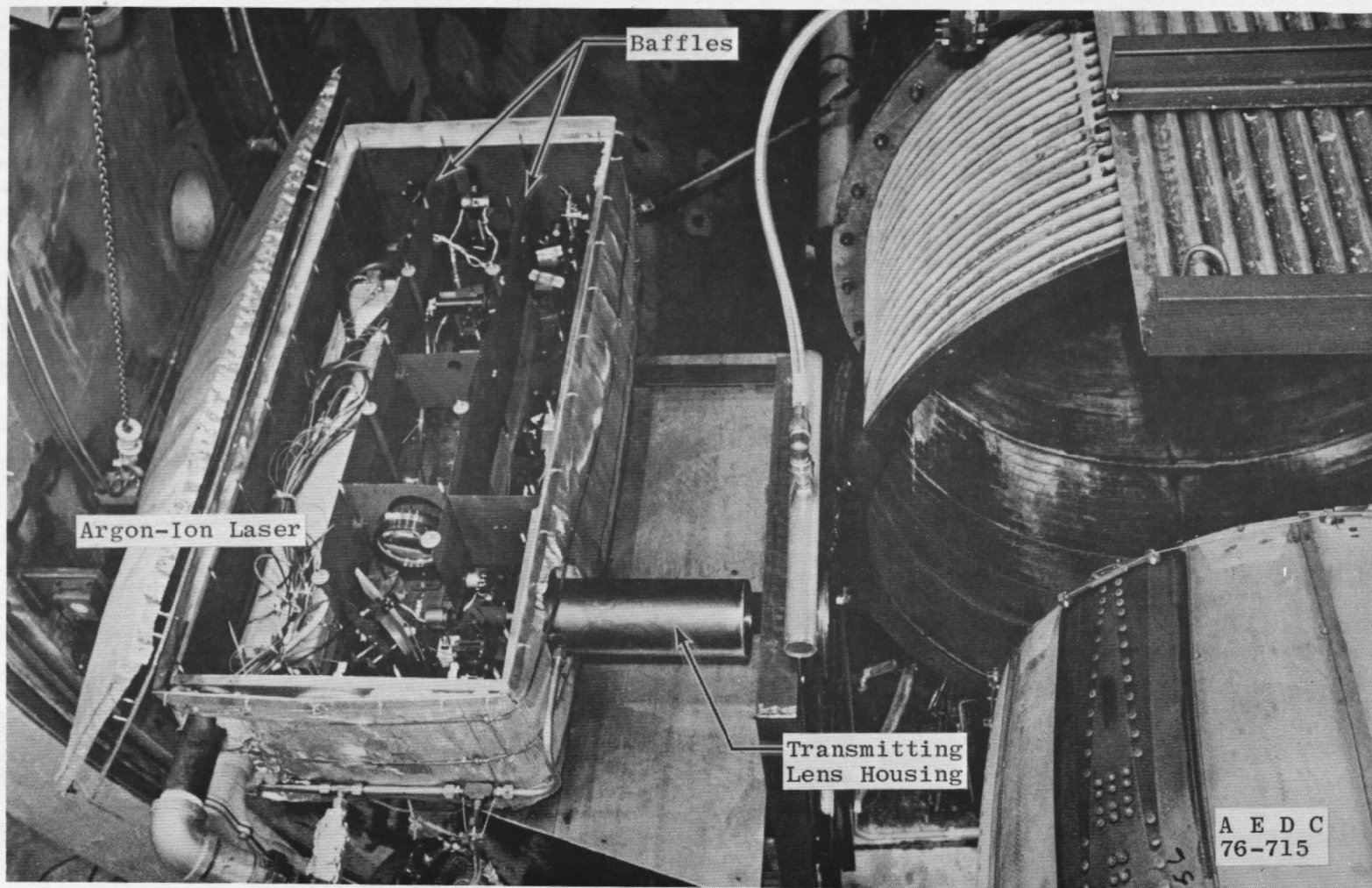


Figure 3. LV/ECS installation.

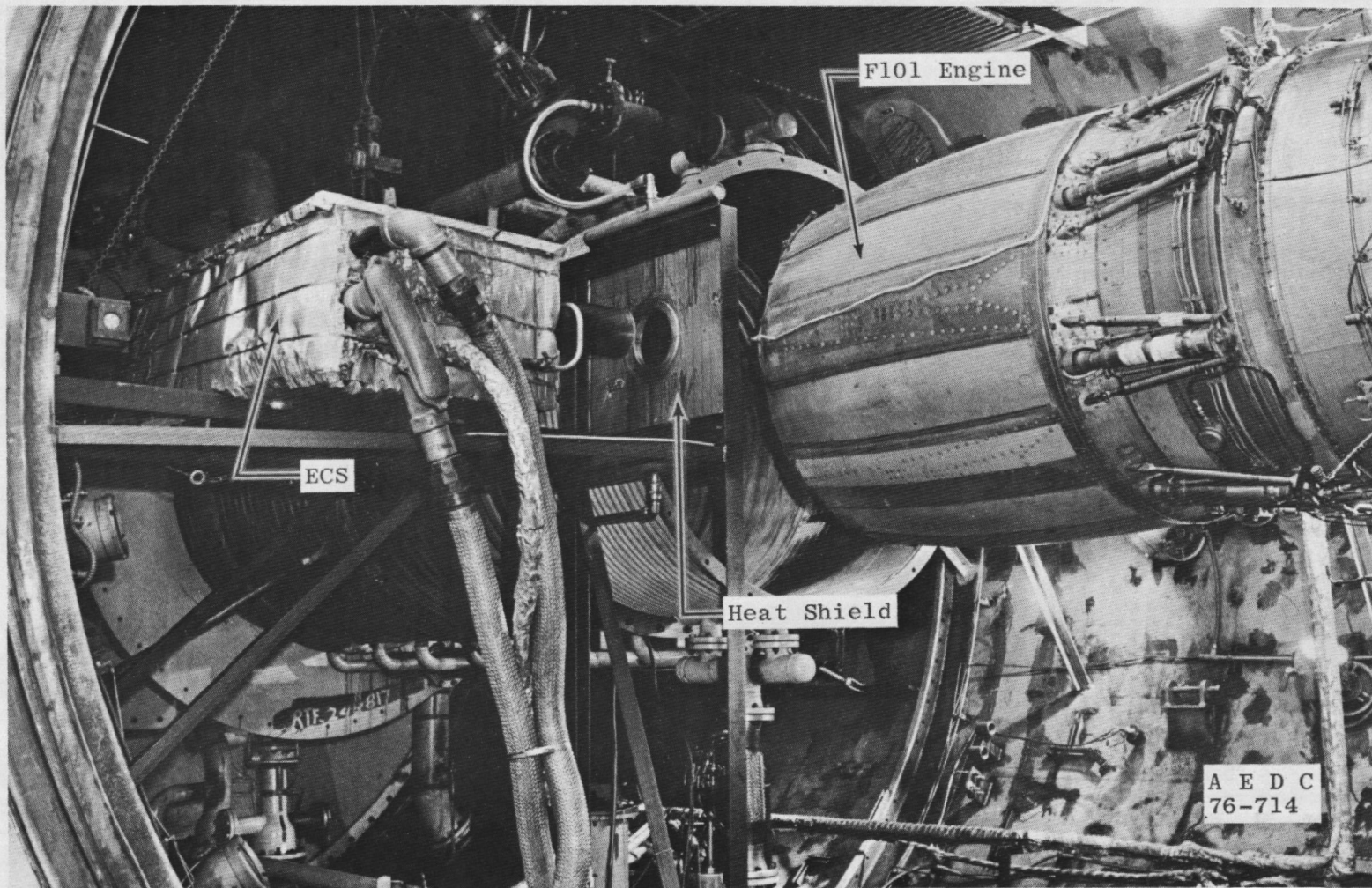


Figure 4. ECS/test cell installation.



The LV system electronics consisted of a preamplifier contained within the ECS and an oscilloscope and Model 8 Doppler Data Processor (DDP) (Ref. 13) located near the engine test cell. Signals from the PMT were amplified and transmitted to the oscilloscope which served as a "trigger" for the data processor by allowing only those signals which exceeded a preset threshold voltage rise to be processed. A signal exceeding the trigger level was amplified and bandpass filtered to enhance its S/N ratio and remove the characteristic low-frequency pedestal associated with Doppler burst data. The resulting periodic signal was converted to a rectangular wave train by a level crossing detector, and the period of eight consecutive cycles of the wave was determined by comparing the total period to that measured by a crystal-controlled clock. Error control logic was provided by the DDP to minimize the acceptance of data having nonperiodic components, high noise content, or in which signal dropout occurred for one or more cycles of the burst. In the Model 8 processors, the periods of four and five cycles of data are compared to 4/8 and 5/8 of the eight-cycle period. Each sample is considered valid only if the processed signal has passed both comparison tests within a tolerance,  $\epsilon$ , of three percent.

The data processors are capable of analyzing signal periods corresponding to one of eight selected frequency bands. For the tests reported herein, the 4- to 20-MHz and 10- to 50-MHz bands were used, giving the LV an approximate velocity range of 200 to 2,900 fps with the 30-in. focal length transmitting lens and 400 to 4,500 fps with the 48-in. lens.

### 2.3 SUPPORTING INSTRUMENTATION

Since one objective of the tests was to determine the effectiveness of the various environmental countermeasures employed to protect the LV system, instrumentation was included in the ECS compartment to measure vibration characteristics and temperature histories and ensure the maintainence of compartment pressure.

Two piezoelectric, triaxial accelerometers were installed at either end of the LV baseplate along a line corresponding to the laser longitudinal axis to monitor vibrations that could cause plasma tube breakage. The x-y axis and relative location of the accelerometers are shown in Fig. 2. The z axis was, therefore, normal to the plane of the baseplate. Each accelerometer had a range of 0 to 1 g with a frequency response of 5 Hz to 10 kHz. The displacement of the baseplate relative to the ECS compartment was measured by two linear potentiometer displacement transducers having a range of  $\pm 0.5$  in. These transducers were located as shown in Fig. 2 and were oriented in different tests to determine displacements along the x or z axis of the accelerometer coordinate system.

Three Chromel®-Alumel® thermocouples were used to measure the free-air temperature in the compartment interior and the temperature of each lens face of the

compound transmitting lens. Each thermocouple had a range of -100 to 600°F. Pressure was a significant variable only in the sense that the laser would malfunction if the compartment pressure dropped below 11 psia. A differential pressure switch was used, therefore, to sound an alarm if the compartment pressure deviated from atmospheric pressure by  $\pm 3$  psi.

## 2.4 DATA ACQUISITION SYSTEMS

Two digital data recording systems were used to acquire data. A computer-controlled data acquisition system (SEL 800) consisting of an SEL-810 computer interfaced to a Raytheon 520 computer and magnetic tape recording module was used to record LV and compartment temperature data. Since the SEL 800 is required to record engine parameters and cell conditions during an engine test, it could not be used to record LV data during engine data acquisition because the potentially high data rates (40,000 samples/sec) possible with the Model 8 DDP would have required dedication of the SEL 800 system to LV data acquisition. An independent data acquisition system consisting of an HP 2100 minicomputer and digital tape recorder was therefore used to record the LV data to be reported concurrently with an established engine data point. The accelerometer and displacement transducer outputs were recorded directly on SEL 800 magnetic tape.

## 2.5 INSTRUMENT UNCERTAINTY

The uncertainty in a velocity measurement made by a stationary fringe laser velocimeter is given by the relation (Ref. 13)

$$\frac{\Delta v_i}{v_i} = \beta + \gamma v_i \quad (1)$$

where  $v_i$  is the velocity of the sample

$$\beta = \frac{\Delta K_v}{K_v} \quad (2)$$

and

$$\gamma = \frac{\Delta r_i}{K_v} \quad (3)$$

It may be further shown that the uncertainty in the velocity-to-frequency conversion is

$$\frac{\Delta K_v}{K_v} = \frac{\Delta L}{L} - \frac{\Delta d}{d} \quad (4)$$

where  $L$  is the distance from the probe volume to a selected measuring plane and  $d$  is the spacing between the two beams at that station. Because of the finite width of the beams and the difficulty in determining the geometric center of the probe volume, it is difficult to determine  $L$  and  $d$  with extreme precision. From the repeatability of measurements, it is estimated that the uncertainty in the distance  $L$  was approximately  $\Delta L = \pm 0.125$  in. and that for  $d$  was approximately  $\Delta d = \pm 0.01$  in. Consequently,  $\beta = \pm 0.014$  for the 30-in. focal length transmitting lens and  $\beta = \pm 0.012$  for the 48-in. lens. The uncertainty in the measurement of period,  $\Delta \tau_1$ , with the Model 8 DDP, was studied in Ref. 10 and may be conservatively estimated to be  $\pm 0.05$  nsec, so that  $\gamma = 8.67 \times 10^{-7}$  sec/ft and  $5.52 \times 10^{-7}$  sec/ft for the shorter and longer focal length lens, respectively. Clearly, for velocities in the range measurable with the present system, the second term of Eq. (1) is negligible, and the uncertainty in velocity measurements with the LV used in the experiments is approximately  $\pm 1.4$  percent for either transmitting lens.

Several other factors contribute to the accuracy of LV measurements including statistical confidence (Ref. 14), statistical bias (Refs. 15 and 16), and particle dynamic effects (Refs. 4 and 10). The confidence in a data set is high for data sets containing many samples and if the turbulence intensity is low. Both criteria are satisfied in the data to be reported. Experiments in both subsonic and supersonic jets (Refs. 10 and 13) have failed to show that statistical bias has a measurable effect on LV data obtained in free-shear flows. While particle lags may produce misleading results in LV measurements of a highly accelerated flow, the velocity gradients expected in the present experiment coupled with the small particles expected in turbojet exhausts (Ref. 5) make it probable that particle dynamic effects did not introduce significant errors in the velocities measured.

## 2.6 TEST PROCEDURES

Prior to each test, functional checks were performed on the supporting instrumentation. The LV was positioned so that the focal point of the transmitting lens and the probe volume coincided with the engine centerline. The access covers to the compartment were then removed, the collector optics aligned, remote alignment detection voltage determined, the fringe spacing measured, and the ECS compartment resealed.

After the test cell was closed, conditioned air was supplied to the engine inlet at the total pressure and temperature that simulated a desired flight condition. Test cell pressure was set at the level necessary to match the desired pressure altitude. In several runs, engine icing tests were performed. For those cases the engine inlet flow was preconditioned to provide a desired liquid water content and mean droplet diameter. Following engine start, the engine performance parameters were stabilized at the throttle setting corresponding to idle operation, and the desired power setting was then set.

During the stabilization period, the LV threshold settings and the optimum DDP frequency range for LV operation were established. LV data acquisition was initiated when the system was, in the opinion of the operator, performing optimally and the engine was sufficiently stabilized at the test condition. An LV data set was completed when 1,000 (or more) individual velocity measurements were made. The time required to acquire a data set varied from a few seconds to several minutes as determined by particle concentration in the exhaust flow, S/N level of the individual signals, and the alignment of the LV at the time when data were acquired. Vibration and temperature measurements for the ECS were recorded only during the engine data acquisition cycle, although temperature was continuously monitored.

## 2.7 DATA REDUCTION

The LV data were reduced using computer codes written for the IBM 370/165 computer. Each raw data tape was read by the digital computer and invalid period samples (indicated by  $\tau_i = 0$ ) were eliminated from the data set. The axial velocity corresponding to each valid period measurement was calculated from

$$V_i = K_v / \tau_i \quad (5)$$

The mean axial velocity was then defined from the arithmetic average of the velocity samples by

$$\bar{V} = \frac{1}{M} \sum_{i=1}^M V_i \quad (6)$$

where  $M$  is the total number of samples. The mean square,  $\overline{V^2}$ , and rms,  $V'$ , values of the axial velocity are determined from

$$\overline{V^2} = \frac{1}{M} \sum_{i=1}^M V_i^2 \quad (7)$$

and

$$V' = \sqrt{\frac{M}{M-1} (\overline{V^2} - \bar{V}^2)} \quad (8)$$

respectively.

A turbulence intensity,  $\sigma$ , is defined as the ratio

$$\sigma = V' / \bar{V} \quad (9)$$

It has been found useful in assessing the validity of LV velocity data (Ref. 10, for example) to examine the distribution of velocities comprising a data set in the form of a histogram or probability distribution. The probability that a given velocity measurement will be found in an interval  $\pm \Delta V/2$  around a value  $V$  is defined as

$$P(V) = \frac{m}{M} \quad (10)$$

where  $m$  is the total number of samples contained in the velocity range  $V \pm \Delta V/2$ . For the data presented,  $\Delta V = 28.9$  fps or 45.9 fps as indicated.

At each engine operating condition, ECS thermocouple outputs were sampled several times, converted to engineering units, and the arithmetic average temperature recorded. Analog data from the accelerometers and displacement transducers were reduced in terms of amplitude-frequency or amplitude-time histories, respectively, with a real time analyzer. Multiplication of the amplitude by an appropriate gain factor gave the desired "g-level" or displacement.

### 3.0 RESULTS AND DISCUSSION

#### 3.1 ENVIRONMENTAL DATA

The ECS was evaluated at test cell altitudes from sea level to 55,000 ft. at engine power settings from idle to maximum thrust augmentor operation. Preliminary data were obtained with the engine operating and the LV simulated by an equivalent mass placed at the instrument's center of gravity to assess the ECS system effectiveness. Following these tests, ECS data were again taken with the LV installed. Only the latter data will be reported.

Two problems related to ECS design were encountered. To make measurements on the centerline of the engine it is, of course, necessary that the transmitting lens be one focal length from that point. For the shorter (30 in.) focal length lens, this required the lens to be located in the plane of the heat shield. In two instances, a transmitter lens was

shattered during low altitude, thrust augmentor operation. The cause for this failure is not certain since either vibration or thermal stressing of the lens could have produced this result. To circumvent this difficulty the lens was replaced with one having a longer (48 in.) focal length so that the ECS compartment could be removed from the proximity of the heat shield. No further breakage resulted after this step was taken. The second problem encountered was that, on several occasions, the compartment pressure dropped to levels that precluded laser operation. In each case, it was clear upon inspection of the ECS that improper sealing of the compartment had permitted the enclosure to vent to the cell ambient pressure.

### 3.1.1 Vibration Data

Typical acceleration-frequency histories obtained during a maximum afterburning engine condition are shown in Figs. 5 through 7 for, respectively, the x (axial), y (transverse), and z (vertical) axes of the LV mounting plate. In each case the acceleration levels are low at low frequencies, as was desired, and the distributions are, generally, characterized by two or more frequency ranges where the accelerations were more severe. These results may be compared qualitatively to measurements made on the test cell wall where the peak accelerations were, approximately,  $a_x = 0.6$  g's,  $a_y = 0.8$  g's, and  $a_z = 0.4$  g's compared to the 0.15 to 0.30 g's experienced by the laser. Clearly, the ECS vibration isolators significantly reduced the forces that would have been experienced by the laser if this protection had not been provided.

A summary of the peak acceleration levels observed at several engine power settings is given in Table 1. It is seen that the severity of the vibrations along all three axes increased as the engine power increased and the traverse accelerations were, in general, the most severe. No significant effect of cell altitude on the results was noted. The displacement gage results are not shown since they simply indicate low-amplitude oscillation of the platform around its equilibrium position. In a few instances, periodic displacements of 0.25 in. or more were seen which are believed to result from "bottoming" of the baseplate on the pneumatic vibration mount. Since this was a random occurrence (in the sense that it could not be correlated with any test conditions), it is probable that this phenomenon resulted from an improper inflation of the mounts.

### 3.1.2 Temperature Data

The ECS internal air temperature and the compound transmitter lens temperatures (forward and aft lens) were continuously monitored and recorded during each engine test condition. The latter results are summarized in Table 2. Compartment temperatures were found to be independent of test conditions, but transmitting lens temperatures increased

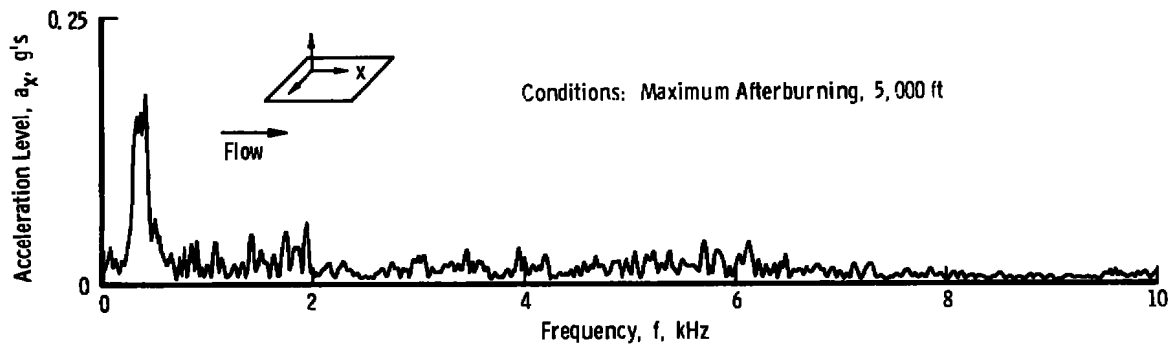


Figure 5. Axial acceleration-frequency distribution.

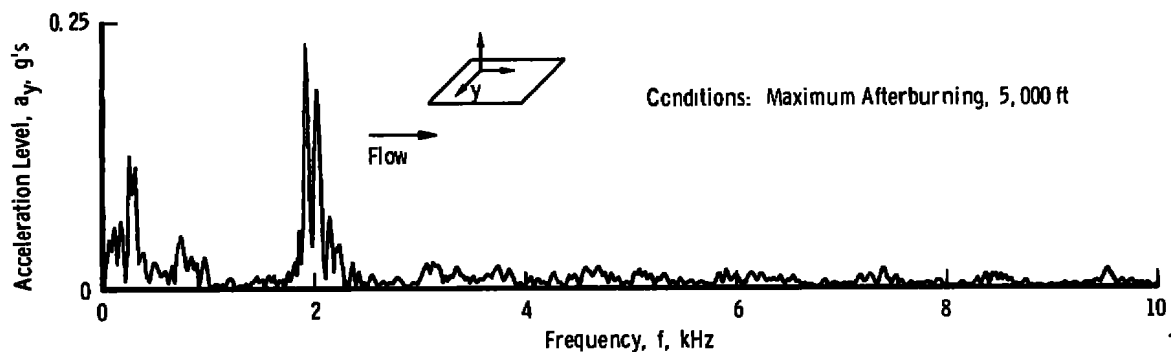


Figure 6. Transverse acceleration-frequency distribution.

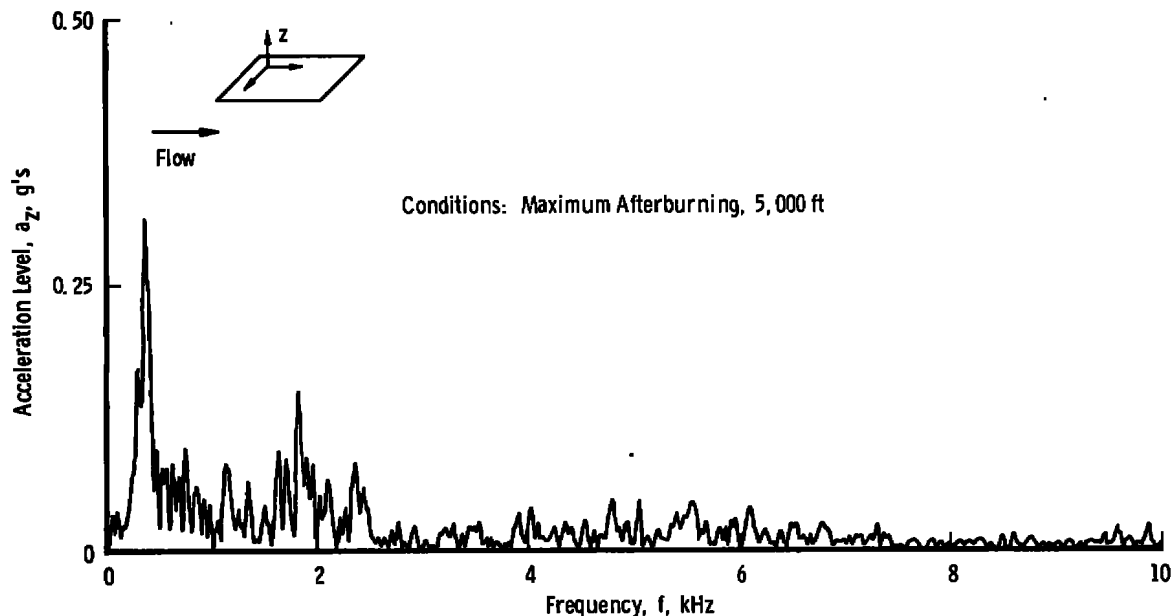


Figure 7. Vertical acceleration-frequency distribution.

Table 1. Maximum Acceleration/Frequency Levels

Test Conditions			Peak Acceleration					
Power Setting	Altitude ft x 10 <sup>-3</sup>	External Mach No.	Longitudinal Axis		Transverse Axis		Vertical Axis	
			a <sub>x</sub> , g's	f, kHz	a <sub>y</sub> , g's	f, kHz	a <sub>z</sub> , g's	f, kHz
Idle	0 to 10	0.3	0.01 to 0.09	0.30 to 0.42	0.02 to 0.10	0.18 to 0.35	0.03 to 0.11	0.19 to 0.31
			0.03 to 0.05	5.7 to 5.8	0.03 to 0.08	1.9 to 2.8	0.03 to 0.05	3.4 to 4.2
Intermediate	0 to 5	0.3	—	—	0.03 to 0.23	0.23 to 0.47	0.02 to 0.19	0.29 to 0.45
			0.02 to 0.04	1.1 to 1.5	0.02 to 0.08	1.0 to 2.2	0.03 to 0.05	1.1 to 2.0
Maximum Thrust Augmentation	0 to 10	0 to 0.3	0.01 to 0.41	0.27 to 0.42	0.05 to 0.30	0.19 to 0.43	0.03 to 0.29	0.21 to 0.55
			0.04 to 0.11	1.0 to 1.5	0.02 to 0.17	1.2 to 1.8	0.05 to 0.15	1.2 to 1.9

Table 2. Lens/ECS Compartment Temperatures

Test Conditions			Temperature Ranges		
Power Setting	Altitude, ft 10 <sup>-3</sup>	External Mach No.	Forward Lens, °F	Rear Lens, °F	Compartment Interior, °F
Idle	0 to 10	0.3	50 to 65	57 to 65	48 to 50
Intermediate	0 to 5	0.3	58 to 75	70 to 80	48 to 70
Afterburning	0 to 10	0 to 0.3	100 to 170	79 to 116	46 to 51



with increases in engine power. None of the observed temperatures is excessive for the LV components. The difference in temperatures between the forward and rear elements of the transmitting lens, however, indicates a strong temperature gradient across the forward lens during afterburning. Since the curved lens was restrained at its edges, this gradient could have introduced thermal stresses which led to the failure of the forward lens element during afterburning tests. As was discussed earlier, lens breakage was eliminated by replacing the 30-in. focal length lens with a 48-in. lens. It should be noted that the range of temperatures observed was strongly dependent on test history since an afterburning test following a series of idle power runs would result in lower ECS temperatures than would be observed when several successive runs were made in a thrust augmentation mode. Consequently, tests having significantly different run sequences could conceivably result in more severe temperature levels.

## **3.2 LASER VELOCIMETER UTILIZATION**

Laser velocimeter measurements of the centerline exhaust velocity were made at a single axial location ( $X = 0.5$  ft) for engine power settings ranging from idle to maximum thrust augmentation at simulated altitudes up to 55,000 ft. Since the F101 engine has a variable exit diameter, the dimensionless axial station varied somewhat, but  $X/D = 0.1$  may be regarded as the nominal axial position of the measurements. During many of the test conditions, insufficient data were acquired to produce statistically meaningful estimates of the mean velocity and turbulence intensity. Accordingly, the LV data to be presented will be confined to those conditions for which the data has a high statistical confidence ( $M > 2,000$  samples). It is noted, however, that an insufficiency of data was the result of data acquisition system malfunctions rather than a lack of particulate matter for obtaining velocity samples.

### **3.2.1 Operational Characteristics**

The LV system was adversely affected by the vibrations within the test cell in that the system collector optics became misaligned after several hours of cell operation. In some cases the system remained aligned for an entire test series, but it could be observed from decreases in the alignment detection voltage that the system was gradually becoming misaligned.

When the alignment was good, the signal quality was excellent and the data rates were high. The signal quality was estimated by visual observation of the Doppler burst signal on the oscilloscope used to trigger the DDP. Typically, the signals showed a classical Doppler burst waveform with low noise level. The signals, thus, were neither photon limited nor subject to excessive noise arising from light scattered by several particles traversing the probe volume simultaneously. Data rates varied with test cell

conditions as well as engine power setting. The maximum observed data rates occurred during engine icing tests and approached 1,000 samples/sec, although a more typical rate for all tests would be an order of magnitude lower.

From the above observations, it is clear that the particle concentration and size distributions in the exhaust flow of the present engine fall within the ranges discussed in Section 1.1. It is, therefore, reasonable to expect that an individual realization LV employing burst counters can yield satisfactory measurements of the engine exit velocity.

### 3.2.2 Velocity Data

The consistency of an LV data set is probably best determined by examining the variation with velocity of the probability function,  $P(V)$ , given by Eq. (10). The mean and rms velocities (defined by Eqs. (7) and (8)) are related to the shape of the resulting histogram since,

$$\bar{V} = \sum_{i=1}^N P(V_i) V_i \quad (11)$$

and

$$V' = \sum_{i=1}^N P(V_i) (V_i - \bar{V})^2 \quad (12)$$

where  $P(V_i)$  and  $V_i$  are evaluated at the center of a velocity band of width  $\Delta V$  and  $N$  is the total number of velocity bands required to span the range of measured velocities.

Typical histograms for the idle, intermediate, and maximum thrust augmentation engine conditions are shown in Figs. 8 through 10, respectively. In each case, the histograms are free of internal inconsistencies which are generally indicative of multiple particle interactions, signal dropout, or electronic noise. The symmetry of the lower power level velocity distributions (Figs. 8 and 9) implies that particle lag effects are not appreciable, although the negative skew of the afterburning case (Fig. 10) may be caused by some particle lag effects. Although these observations are qualitative, they indicate that the LV measurements are self-consistent and of good quality. An interesting facet of the measurements is that the turbulence intensity on the nozzle centerline is relatively low and increases only slightly as the engine power is increased.

An obvious difficulty in assessing the validity of the LV results is the absence of measurements of the mean axial velocity of the F101 engine. In order to qualitatively determine the centerline velocity and provide a basis for comparison, two approximate

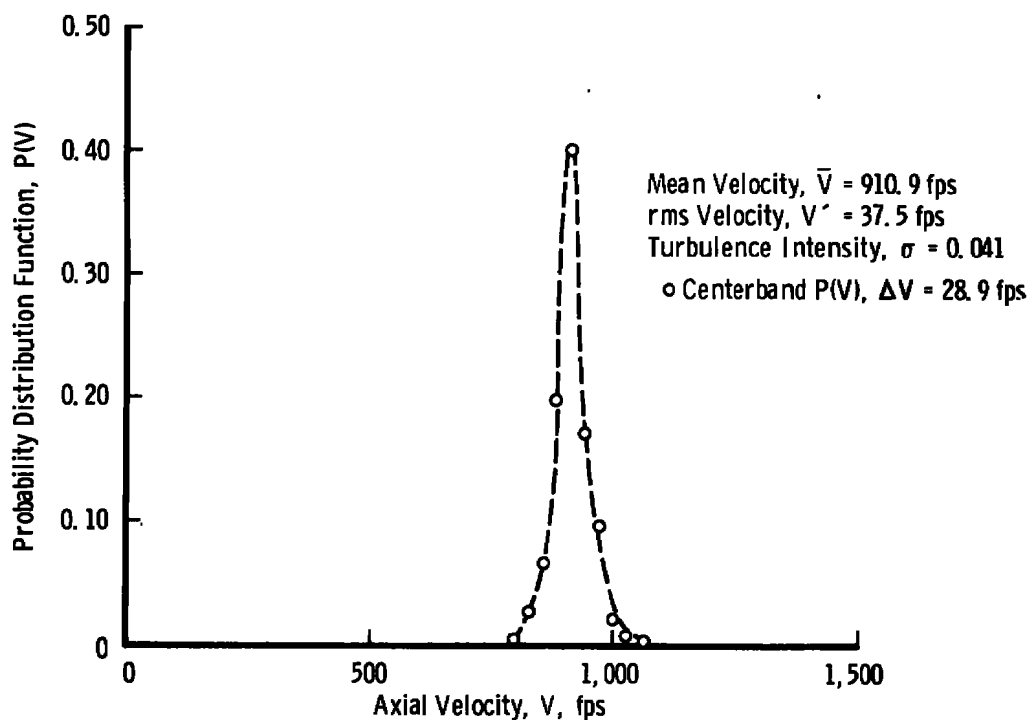


Figure 8. Exit velocity histogram for engine idle.

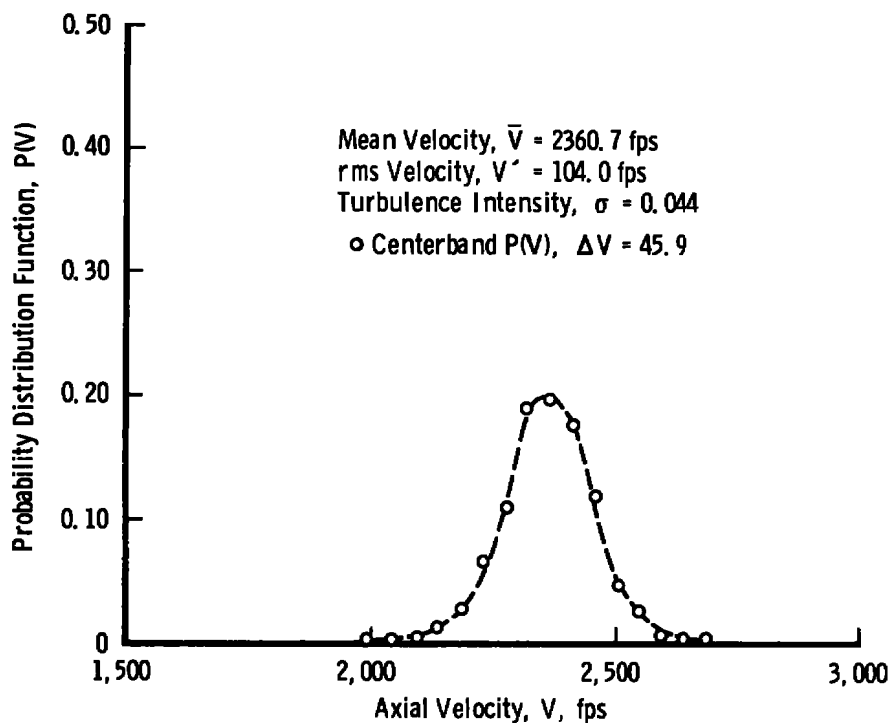


Figure 9. Exit velocity histogram for intermediate power.

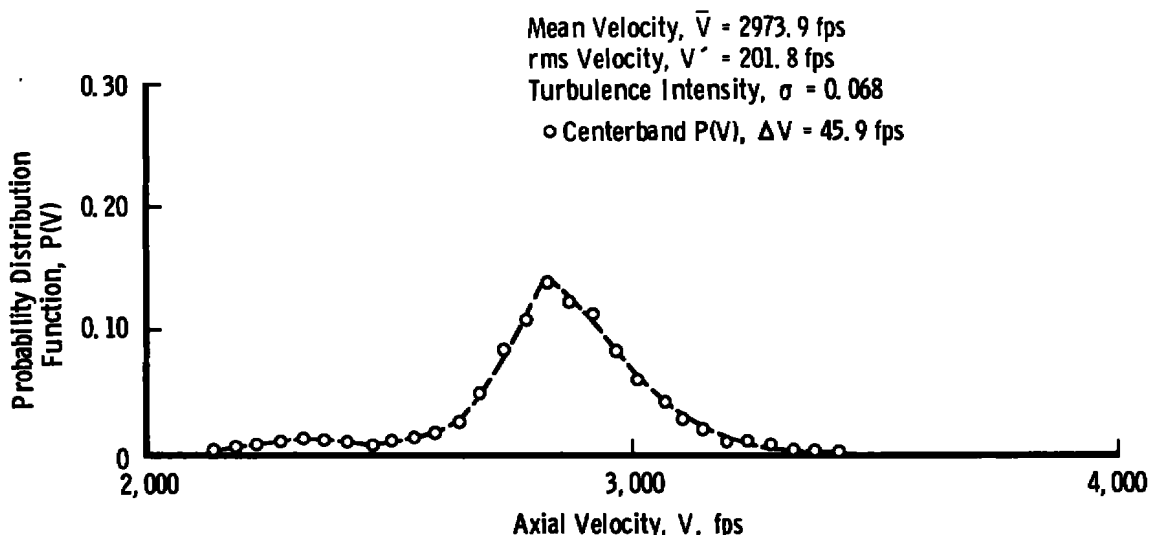


Figure 10. Exit velocity histogram for maximum thrust augmentation.

calculations were made. The first technique used engine pressure and temperature measurements to determine a one-dimensional exit velocity,  $V_I$ , for the engine. For this calculation, the Mach number and static temperature distributions across the nozzle were assumed constant. A second approach was to use existing development data on the nozzle throat total-temperature distributions and assume they were identical to the exit plane temperature distributions. Assuming a constant exit Mach number (again determined from the nozzle pressure ratio), it was then possible to evaluate the static temperature distribution at the exit plane. A centerline exit velocity,  $V_c$ , could then be calculated for the intermediate and maximum reheat conditions for which total temperatures were available.

A comparison of several LV measurements of the centerline exit velocity,  $\bar{V}$ , to the computed values is presented in Table 3. Also shown in Table 3 is the velocity difference,  $\epsilon_v$ , computed from

$$\epsilon_v = \left| \frac{V_{calc} - \bar{V}}{\frac{1}{2}(V_{calc} + \bar{V})} \right|$$

where  $V_{calc}$  is the appropriate calculated exit velocity. It is seen that the measured and calculated values differ from one another, in the best cases, by three to six percent. In view of the approximations inherent in the calculations of the exit velocity, this is encouraging.

**Table 3. Comparison of Measured and Computed Mean Velocities**

Test Conditions		Measured Velocity, $\bar{V}$ , fps	Computed Exit Velocity			
Power Setting	Altitude Range, ft x 10 <sup>-3</sup>		Method I $\bar{V}_I$ , fps	Difference, $\epsilon_v$ , percent	Method II $\bar{V}_C$ , fps	Difference, $\epsilon_v$ , percent
Idle	0 to 10	908.4	944.1	3.8	—	—
Intermediate	25 to 40	2353.0	1869.9	22.9	2208.6	6.3
Thrust Augmentation	25 to 40	2974.6	3318.2	10.9	2881.5	3.2

#### 4.0 CONCLUSIONS

A laser velocimeter was successfully used to determine the centerline exit velocity and turbulence intensity of a turbofan engine installed in an altitude test cell. The observed data rates were sufficiently high to show that LV measurements of velocity are possible during steady-state engine operation using only natural particulates contained in the exhaust flow. It is inferred, from the observed signal, that the particle size range was adequate for utilizing conventional doppler data processors.

The ECS designed to protect the LV optics from the extreme vibration and temperature levels present during engine tests performed satisfactorily, although several deficiencies in the prototype protection system were noted. Of primary concern was the structural failure of the transmitting lens during maximum thrust augmentation operation of the engine. Since the cause of this failure could be attributed to either vibration or thermal stresses induced in the lens, future ECS designs must consider improved vibration isolation of the lens as well as thermal protection systems designed to minimize the temperature gradient through the lens. Two other needed improvements indicated are (1) a means to assure that the vibration isolators are properly inflated throughout a test and thus avoid "bottoming" of the baseplate and (2) improved sealing of the ECS compartment to prevent loss of pressure during high-altitude tests.

The alignment detection system proved to be invaluable in determining whether proper alignment was maintained but provided no means for correcting deficiencies in alignment. Future LV systems to be used in acquiring engine test data should, therefore, have provisions for remote optical alignment of the collector optics. For the LV to achieve its full potential in engine testing, future systems must have a remote traversing capability so that velocity distributions across the flow can be obtained during the course of the engine data acquisition cycle.

## REFERENCES

1. Pfeifer, H. J. and Haertig, J., Editors. "Proceedings of the ISL/AGARD Workshop on Laser Anemometry." German-French Research Institute Report R117/76, St. Louis, France, June 1976.
2. Eckert, E. R. G., Editor. "Minnesota Symposium on Laser Anemometry." University of Minnesota, St. Paul, Minnesota, January 1976.
3. Thompson, H. D. and Stevenson, W. H., Editors. "Second International Workshop on Laser Velocimetry." Purdue University Engineering Experiment Station Bulletin No. 144, W. Lafayette, Indiana, 1974.
4. Hsieh, T. "Analysis of Velocity Measurements about a Hemisphere-Cylinder Using a Laser Velocimeter." Journal of Spacecraft and Rockets, April 1977.
5. Broderick, A. J. "Particles in High-Altitude Aircraft Exhaust." Proceedings of the Third Conference on the Climatic Impact Assessment Program, DOT Report DOT-TSC-OST-74-15, March 1974.
6. Mayo, W. T. "Modeling Laser Velocimeter Signals as Triply Stochastic Poisson Processes." Minnesota Symposium on Laser Anemometry, 1976.
7. Smart, A. E. and Moore, C. J. "Aero-Engine Applications of Laser Anemometry." AIAA Journal, Vol. 14, No. 3, March 1976.
8. Norgren, C. T. and Ingebo, R. D. "Particulate Exhaust Emissions from an Experimental Combustor." NASA TMX-3254, June 1975.
9. Lennert, A. E., Brayton, D. B., and Crosswy, F. L. "Summary Report of the Development of a Laser Velocimeter to be Used in AEDC Wind Tunnels." AEDC-TR-70-101 (AD871321), July 1970.
10. Barnett, D. O. and Giel, T. V., Jr. "Laser Velocimeter Measurements in Moderately Heated Jet Flows." AEDC-TR-76-156.
11. "Test Facilities Handbook (Tenth Edition). "Engine Test Facility, Vol. 2." Arnold Engineering Development Center, May 1974.

12. Brayton, D. B. and Goethert, W. H. "A New Dual-Scatter Laser Doppler-Shift Velocity Measuring Technique." ISA Transactions, Vol. 10, No. 1, 1971.
13. Barnett, D. O. and Giel, T. V., Jr. "Application of a Two-Component Bragg-Diffracted Laser Velocimeter to Turbulence Measurements in a Subsonic Jet." AEDC-TR-76-36 (ADA025355), May 1976.
14. Cline, V. A. and Bentley, H. T., III. "Application of a Dual Beam Laser Velocimeter to Turbulent Flow Measurements." AEDC-TR-74-56 (AD785352), September 1974.
15. McLaughlin, D. K. and Tiederman, W. G. "Biasing Correction for Individual Realization Laser Anemometry Measurements in Turbulent Flows." Physics of Fluids, Vol. 16, No. 12, December 1973, pp. 2,082-2088.
16. Barnett, D. O. and Bentley, H. T., III. "Statistical Bias of Individual Realization Laser Velocimeters." Proceeding of the Second International Workshop on Laser Velocimeter, Purdue University Engineering Experiment Station, Bulletin No. 144, March 1974, pp. 428-444.

## APPENDIX A

### LV ALIGNMENT CHARACTERISTICS

The general operating characteristics of the LV are described in Sections 2.2 and 2.6. This Appendix provides additional details on the system's initial optical alignment and remote alignment detection features as well as the optical baffling of the LV.

Figure A-1 is a schematic of the LV optical and alignment system. The following symbol identification applies to Fig. A-1 and the discussion which follows.

<u>Symbol</u>	<u>Description</u>
B1, B2	Cylindrical baffle tubes
B3 through B7	Flate plate baffle
BE	Beam expander
BS	Beam splitter
CC	Corner cube (retroreflector)
DF1, DF2	Neutral density filter
1, 1a, 2a, etc.	Beam identification
L <sub>1</sub> , L <sub>2</sub>	Lens
LLF	Laser line filter
M <sub>1</sub> , M <sub>2</sub>	Mirrors
M <sub>3</sub>	Partial mirror
PH	Pinhole
PMT	Photomultiplier tube
(→)	Displacement required to affect alignment

Optical alignment is initiated by inserting DF1 to attenuate the laser beam and placing the scatter plate at the center of the probe volume. The surfaces of DF1 are flat and parallel. Light scattered from the scatter plate is focused onto the pinhole (PH) by L<sub>1</sub>, M<sub>4</sub>, and L<sub>2</sub>. The large angle of the light cone between L<sub>2</sub> and the PH provides an image with very little depth of field and thereby allows very precise longitudinal (X-axis) positioning of the PH. Mirror M<sub>4</sub>, which can be tilted about two orthogonal axes, is then positioned to center the scatter plate image onto the pinhole.



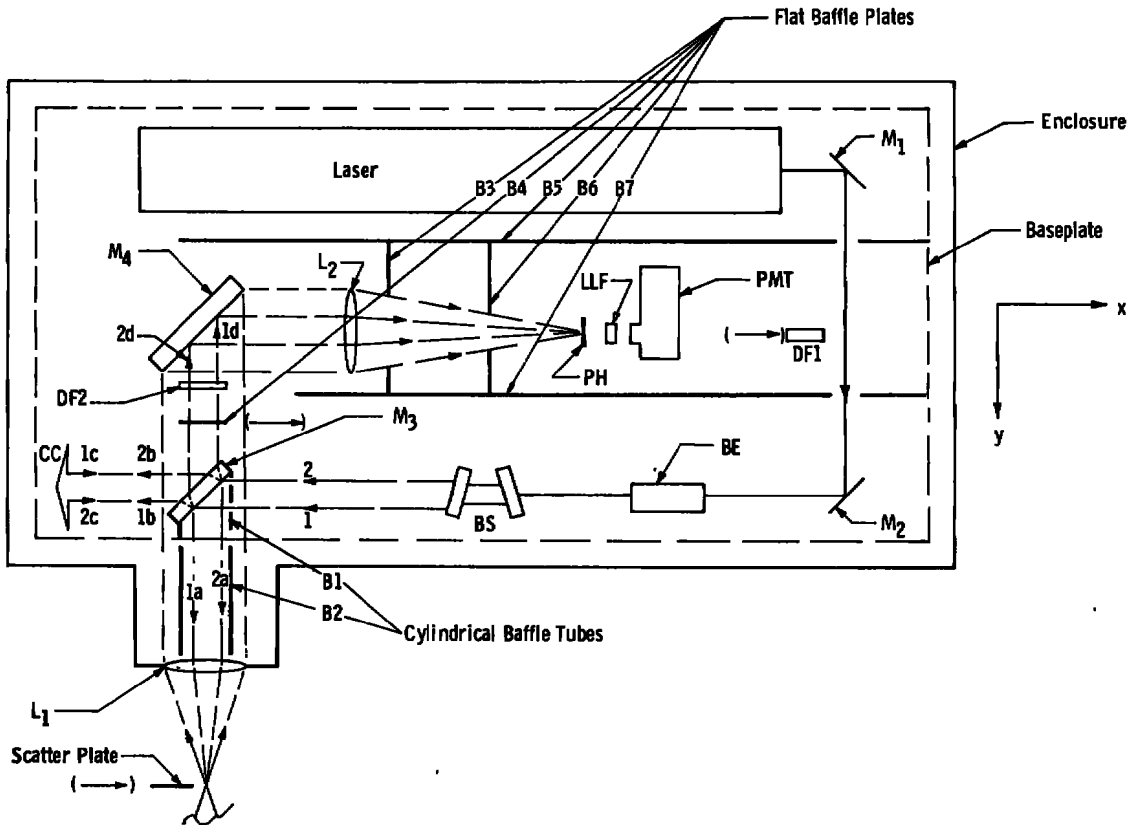


Figure A-1. LV optical and alignment system.

Alignment detection is achieved remotely by actuating a solenoid that causes baffle plate B4 to move to the right, thus allowing the reference beams 1d and 2d to focus on the pinhole. Once the initial optical alignment is achieved through use of the scatter plate, the optical design is such that the reference beams will also focus on the pinhole. Movement of one or more optical elements, the laser,  $M_1$ ,  $M_2$ , BE,  $M_3$ ,  $M_4$ , or PH, that can cause misalignment of the scatter plate image on the pinhole will also cause an identical misalignment of the focus of the reference beams on the PH. The reference beam power level, remotely detected by the photomultiplier tube (PMT), therefore, is used as a quantitative measure of the degree of optical alignment.

The attainment of alignment detection through the use of reference beams was accomplished as follows. The parallel and collimated beams 1 and 2 are partially transmitted through (via beams 1b and 2b) the 99-percent reflective front face of the partial mirror  $M_3$ . Beams 1b and 2b are reflected back parallel (via beams 1c and 2c) to the incident beams by the corner cube (CC). Beams 1c and 2c then reflect off  $M_3$  thereby generating beams 1d and 2d which are parallel to beams 1a and 2a. The flatness

and parallelism of the front and back faces of both  $M_3$  and DF2, together with the accuracy of CC and the flatness of  $M_4$ , ensure that beams 1d and 2d are parallel to beams 1a and 2a. Since rays 1a, 2a, 1d, and 2d are parallel to the backscattered rays (from the scatter plate or the probe volume) collimated by lens  $L_1$ , these rays will be focused by lens  $L_2$  to the same spot. It should be noted that displacement of lens  $L_1$  (mechanically mounted to the enclosure) relative to the remaining optical components (mechanically mounted to the base plate and vibration isolated from the enclosure) will not misalign the system.

The baffling shown in Fig. A-1 was necessary to reduce the background radiation (that not received from the probe volume) to a negligible value. The scattered light from points at which the high-power beams (those emitted from the laser and beams 1, 2, 1a, and 2a) intercept the optical elements and other extraneous reflections are of primary concern. Such light must be substantially attenuated before portions of it eventually reach the pinhole to obtain a high signal-to-noise ratio. This is accomplished by causing such reflections to follow a very complicated path involving a number of secondary scatterings from the highly absorbent baffle plates.

## NOMENCLATURE

### GENERAL

<b>a</b>	Semi-major axis of probe volume, mm
<b><math>a_x, a_y, a_z</math></b>	Acceleration along the x, y, and z coordinate axes, g's
<b>b</b>	Semi-minor axis of probe volume, mm
<b>D</b>	Exit diameter of test engine, ft
<b>d</b>	Distance between beams of calibration plane, in.
<b><math>d_p</math></b>	Particle diameter, $\mu\text{m}$
<b>ECS</b>	Environmental control system
<b>e</b>	Transcendental logarithmic base, 2.71828...
<b>f</b>	Frequency, Hz
<b>g</b>	Acceleration of gravity, $\text{ft/sec}^2$
<b><math>K_v</math></b>	Velocity-to-frequency conversion ratio, $\text{fps/MHz}$
<b>L</b>	Distance from probe volume to calibration plane, in.
<b>LV</b>	Laser velocimeter
<b>M</b>	Total number of samples in data set
<b>m</b>	Number of samples contained in velocity interval $\Delta V$
<b>N</b>	Number of velocity intervals in range of data
<b><math>P(V)</math></b>	Probability that sample will be found in the interval $V \pm \Delta V/2$
<b>S/N</b>	Signal-to-noise ratio
<b>V</b>	Velocity, fps
<b>X</b>	Axial station measured from nozzle exit plane, ft
<b>x,y,z,</b>	Mounting plate longitudinal, traverse, and vertical axes

$(\beta, \gamma)$	Error coefficients in uncertainty analyses
$\Delta$	Difference
$\delta$	Fringe spacing, $\mu\text{m}$
$\epsilon$	Tolerance used in Model 8 DDP error detection logic
$\epsilon_v$	Difference in computed and measured mean velocities
$\sigma$	Turbulence intensity
$\tau$	Period of measurement

#### STATISTICAL PARAMETERS

$\bar{V}$	Mean velocity
$\overline{V^2}$	Mean square velocity
$\bar{V}'$	Root-mean-square velocity

#### SUBSCRIPTS

calc	Calculated
c	Computed value for centerline
i	$i^{\text{th}}$ sample
l	Computed one-dimensional value